한국마린엔지니어링학회지 제34권 제5호, pp. 686~694, 2010. 7 (ISSN 1226-9549)
Journal of the Korean Society of Marine Engineering

Evaluation of the Damage Mechanism in CFRP Composite Using Computer Vision

Oh-Heon Kwon† · Shaowen Xu[1] · Michael Sutton[2]

(Received May 18, 2010; Revised June 9, 2010; Accepted June 9, 2010)

Abstract: Continuing progress in high technology has created numerous industrial applications for new advanced composite materials. Among these materials, carbon fiber-reinforced plastic (CFRP) laminate composite is typically used for low-weight carrying structures that require high specific strength. In this study, the damage mechanism of a compact tension (CT) specimen of woven CFRP laminates is described in terms of strain and displacement changes and crack growth behavior. The digital image correlation (DIC) method (which is employed here as a computer vision technique) is analyzed. Acoustic emission (AE) characteristics are also acquired during fracture tests. The results demonstrate the usefulness of these methods in evaluating the damage mechanism for woven CFRP laminate composites.

From the results, we show these methods are so useful in order to evaluate the damage mechanism for woven CFRP laminate composites.

Key words: Damage mechanism; Digital image correlation; Strain contour; Woven CFRP composite, Acoustic emission

1. Introduction

In recent years, new advanced composite materials have found their way into a wide range of industrial applications. Among these composite materials, carbon fiber-reinforced plastic (CFRP) laminate is typically used for low-weight carrying structures with high specific strength. The overall weight of the main body of an aircraft could be considerably reduced by the adoption of CFRP. However, CFRP composites are subject to several types of damage, including delamination, interfacial matrix/fiber debonding, transverse and matrix micro cracking, and fiber pullout. These phenomena lead to complex assessment mechanisms. Moreover, in the case of a woven composite (which has a non-uniform surface structure), damage-causing behavior often cannot be readily described. A considerable amount of research has already been devoted to understanding unidirectional ply damage [1].

However, woven ply characteristics are not as well understood, especially with regards to the damage mechanisms. Harry and Massard [2] used the Tsai-Wu

† Corresponding Author(Division of Safety Engineering, Pukyong National University, E-mail: kwon@pknu.ac.kr, Tel: 051)629-6469)
1 Department of METEET, Geogia Southern University, USA
2 Department of Mechanical Engineering, University of South Carolina, USA

quadratic criterion to examine woven ply characteristics; however, this technique requires the warp and fill characteristics of a woven CFRP laminate composite. Le'ne' and Paumelle [3] examined the state of the stress in a woven ply. Gao et al. [4] observed the behavior of woven-fabric laminates under monotonic loading.

In this work, the damage mechanism of a CT specimen of woven CFRP laminates under tension loading is described in terms of strain and deformation changes and crack growth behavior. To accomplish this, the digital image correlation (DIC) technique is employed as a computer vision method. Acoustic emission (AE) characteristics are also acquired during fracture tests.

Digital image correlation (DIC) is a powerful tool for strain field measurement because it can be used to map strain distributions over a whole area of machinery and structures. DIC analysis is based on the recognition of changes in the grayscale distribution of speckled surface area patterns before and after deformation. Automatic and non-contact measurement can be carried out via a simple DIC experimental apparatus. Sutton et al. [5], who developed DIC from traditional speckle photography techniques, estimated crack growth and crack blunting in thin 304 SUS SEC specimens with various crack ratios.

Until now, DIC techniques have been applied almost exclusively to homogeneous materials. We have attempted to evaluate the behavior of woven CFRP laminate composites by using DIC as a computer vision technique.

From the results, we show that the woven CFRP fracture damage mechanism and strain fields are well expressed by DIC method and AE measurement.

2. Experimental Method

2.1 Materials and Specimen

The materials used in this research are laminates of woven, epoxy-sized carbon fiber-reinforced prepregs (CF3327EPC with a thickness of 0.27 mm and a fiber weight of 205g/m^2) in the form of six-layer laminates, normally containing 60% fibers by volume. In the laminates, the plies are arranged symmetrically around the middle plane. The fiber cloths in the materials are plain-woven, and have an identical filament count in the warp and weft yarns. (Warp refers to lengthwise threads, which run the length of the roll of woven cloth, and weft refers to transverse or crosswise threads woven into the warp threads.) The plain-woven prepregs are stacked symmetrically about the middle line. Figure 1 shows a scanning electron microscopy (SEM) image of a section of the laminate. Figure 2 shows a photograph of the reinforced carbon fiber diameter, also obtained by SEM. The volume fraction of the fibers can be estimated by Equation (1), in which the area of interest is 0.25 mm by 0.25 mm.

$$V_f = \frac{W_f/\rho_f}{W_f/\rho_f + (1-W_f)/\rho_m} \quad (1)$$

where W_f, ρ_f and ρ_m are the fiber weight, fiber density and matrix density, respectively. In this study, the volume fraction of the fiber is about 56%. The

respective values of ρ_f and ρ_m are 1.75 g/cm^3 and 1.4g/cm^3.

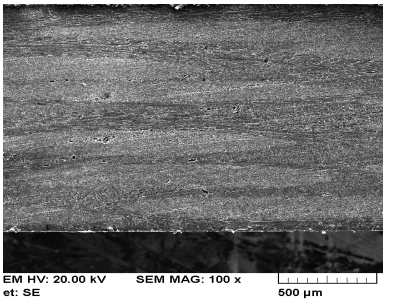

Figure 1: SEM image of a section of the plain-woven CFRP laminate.

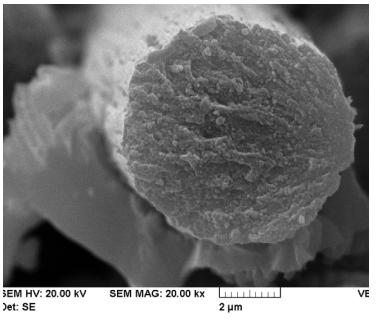

Figure 2: Photograph of a carbon fiber diameter.

Six prepreg plies were laminated in a hot press (50 MPa, Due. Co.) at a controlled temperature of 140°C and gauge pressure of 6 MPa. The thickness of the fabricated plain woven CFRP composite was 1mm. Specimens were cut in 0° direction relative to the loading orientation(Θ=0°). Tensile and compact tension(CT) specimens were fabricated with a diamond wheel fine-cutting machine. To reduce slippage and damage caused by the tester grips, an aluminum end tab was adhered to both sides of the tensile specimen end, and heat treatment was performed in an electric furnace (K. Co. HY-8000s) at 80°C for 30minutes.

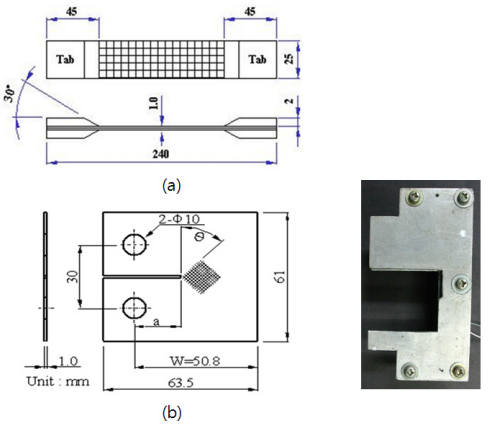

Figure 3: Geometry of a (a) tensile specimen and (b) CT specimen with an anti-buckling jig.

An anti-buckling jig was attached to the CT specimen to eliminate the buckling effects caused by the thinness of the specimen, as shown in Figure 3. Tensile properties were measured in accordance with the ASTM D3039-00. Mode I fracture behavior was studied using the CT specimen. A starter notch for an initial crack tip was cut into the CT specimen with a razor blade. The radius of curvature of this notch was very small. The width of the notch was 0.5mm and the initial crack length a_0 to specimen width W, ratio a_0/W was 0.6. The tensile and fracture test of the CT specimen were carried out under a displacement control of 0.2mm/min at room temperature.

Prior to conducting to the DIC test, the specimen was slightly sprayed with fine white acrylic resin- based paint. A fine pattern of black dots was then sprayed onto the fully dried white surface to obtain random speckles. The surface quality of a specimen with original images is the one of the key factors that determine the quality of the results

obtained from DIC method. The optimum quantity and size of the spray droplets, shadowing effects, and overall illumination are important factors to be taken into account before imaging sample surface. Figure 4 shows the CT specimen with random speckle patterns.

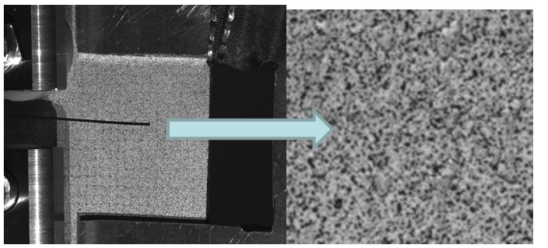

Figure 4: Random speckles sprayed onto the surface of a CT specimen with white and black paint.

2.2 Digital Image Correlation (DIC)

A brief description of the DIC method is given here. More details can be found in the literature[5]. Consider a planar body undergoing a two-dimensional deformation, such as the one shown in Figure 5.

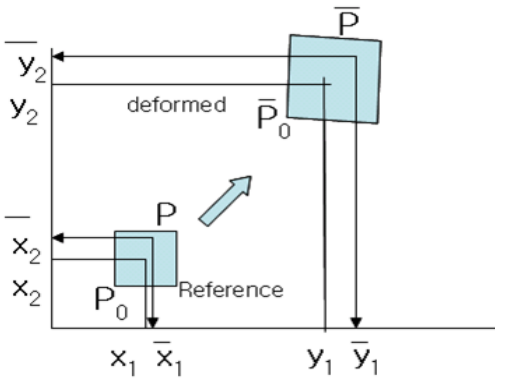

Figure 5: A schematic local DIC region deformation under loading.

The material point P_0 at coordinate (x_1,x_2) in the undeformed configuration is shifted to the coordinate(y_1,y_2) by the deformation. If we consider a point P at the coordinates$(\overline{x_1},\overline{x_2})$ in the subset S, and if S is small enough for the deformation to be locally homogeneous around P_0, then;

$$\overline{y_1}=\overline{x_1}+u_1+u_{1,1}\triangle x_1+u_{1,2}\triangle x_2 \quad (2)$$
$$\overline{y_2}=\overline{x_2}+u_2+u_{2,1}\triangle x_1+u_{2,2}\triangle x_2$$

where u_1 and u_2 are the displacement of $P_0(x_1,x_2)$ in direction 1 and 2, respectively, $u_{\alpha,\beta}$ denotes the differential $\partial u_\alpha/\partial x_\beta$ and $\triangle x_\alpha=\overline{x_\alpha}-x_\alpha,\alpha=1,2$.

Originally the DIC method employed a two-dimensional correlation of deformed and undeformed images of subsets of the region of interest(ROI) to determine the deformation field of the surface and obtain the six parameters $u_1,u_2,u_{1,1},u_{1,2},u_{2,1},u_{2,2}$ in Equation(2). Since a pixel in the undeformed image may be displaced to a non-pixel point in the deformed configuration, an estimation is used to obtain the gray level intensity at a point (y_1,y_2) that does not appear on the rectangular grid of the deformed image. The gray scale intensity is obtained by interpolation from the known intensities at the pixel points of the deformed image. The bilinear interpolation function is used for this purpose. After interpolation, the pixel intensities of the undeformed and deformed images are compared to each other. The values of the six parameters $V=(u_1,u_2,u_{1,1},u_{1,2},u_{2,1},u_{2,2})$ are obtained by minimizing the correlation coefficient using the Newton-Raphson(NR) method developed by Sutton et al.[5]. This method involves simultaneous minimization of all six parameters.

2.3 Experimental Procedure

The experimental apparatus used for the fracture test consisted of a 250kN servo-hydraulic MTS testing machine and two charge-coupled device(CCD) cameras connected to a personal computer(PC), which was used to record images of the specimen surface. An AE sensor was attached to the surface of the specimen. Following data acquisition, the images and load-displacements were transferred to the PC, on which the DIC software was implemented. Three-dimensional stereo images were taken using two 8-bit QImaging QIcam digital cameras with a CCD resolution of 1360 by 1036 pixels.

The AE characteristics were obtained by the PC system via an AE-DSP32 board(PAC Co.). During AE evaluation, the threshold type was as set as fixed, and the value was set at 46dB in the fracture test and 22dB in the tensile test. An R15 AE sensor was used, along with a band filter with a range of 100kHz to 300kHz. The AE data were analyzed using AE software MISTRAS2001. The crack length was measured by a traveling microscope, and the surface damage was examined Also the strain gage was attached to the back surface of the tensile and CT specimen, respectively. The strain gauge was attached to the center of the specimen in the case of tensile test, and at horizontal distance of a 5mm from the crack tip of the CT specimen. The values obtained from the strain gauge were compared with the results from the DIC analysis to validate the DIC techniques.

3. Results and Discussion

3.1 Mechanical Property Measurement

The global stress and strain curve obtained from the tensile test is shown in Figure 6. The curve increased linearly up to the fracture. In the type of materials used, the woven fibers crossed each other orthogonally, and the weft direction was oriented parallel to the tensile loading axis. The identical behavior of the warp and weft fiber orientations was consistent with the symmetry of the sample. The woven CFRP composite showed the maximum tensile strength of the fibers because the fracture behavior was controlled by the reinforcing fibers with high strength. Also, the CFRP composite material showed high fracture strength and low ductility because the epoxy resin matrix was much weaker than the fibers. Thus, the epoxy resin matrix alone could not bear the applied load, and failed without plastic behavior. Such behavior can be manifested as a heterogeneous strain map obtained by DIC analysis.

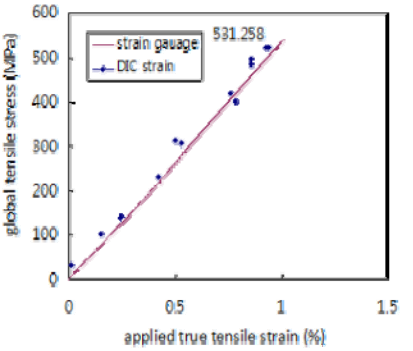

Figure 6: Global stress-strain behavior curve.

The ϵ_{yy} strain obtained by DIC at the center of the specimen was about 1.0%.

This value as almost the same as the strain recorded by the strain gauge measurement system(Scanner 5100B)on the back face of the specimen. For the sake of comparison, the strain values obtained from the strain gauge measurement system and DIC are both shown in Figure 6. The values are virtually identical. The maximum strain at the last step(95.4% loading rate) was about 2% on the corner of left side, where the damage was greatest. The mechanical properties obtained from the tensile test are listed in Table 1.

Table 1: Mechanical properties for the woven CFRP laminate under the tensile test.

Tensile Modulus E	52 GPa
Ultimate Strength	531 MPa
Failure strain	1.0%
Poisson Ratio	0.1

3.2 Fracture test with CT specimen

Figure 7 shows the load-displacement relation and the AE counts for CT specimen. The images were taken several times at each load step for DIC analysis.

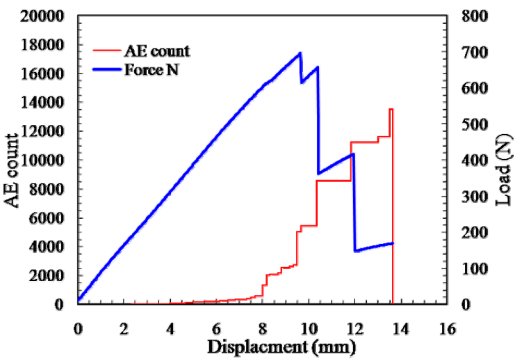

Figure 7: Load-displacement and AE count variation from the CT specimen fracture test.

The maximum load occurred at the 9th step. The first micro damage appeared between 5th and 6th load steps, where the AE counts increased sharply 1308 and 2073.

The first crack was initiated at the maximum load point, followed by a sharply decreasing load, and the AE count increased rapidly to 5412. After the appearance of the first crack at the maximum load, the crack advanced discontinuously at each step. The final AE count at the fracture was about 13500. Since the resistance of the fiber bundle oriented in the notch direction was weaker than that of the perpendicular fiber bundle, the crack extended easily in the warp fiber direction, even under high load. Thus the AE count rose sharply to the 5412, although this value is not especially high. When the crack advanced in the direction perpendicular to the fiber bundle, many fibers were damaged and broken, and a zigzag path occurred in one area of the fiber bundle. This situation corresponds to higher AE count characteristics. And the all strain contours over the whole area of interest were evaluated by DIC analysis. The strain contours ϵ_{yy} at each step are shown in Figure 8. The maximum normal strain ϵ_{yy} (at load step 11, after cracking) was 0.00531.

We can find the relationship between the AE count and maximum normal strain ϵ_{yy} from the DIC analysis, as shown in Figure 9. The tendency curve from this relationship is Equation(3).

$$\epsilon = 0.001\ln(C_{AE}) - 0.003 \quad (3)$$

where C_{AE} is the AE count.

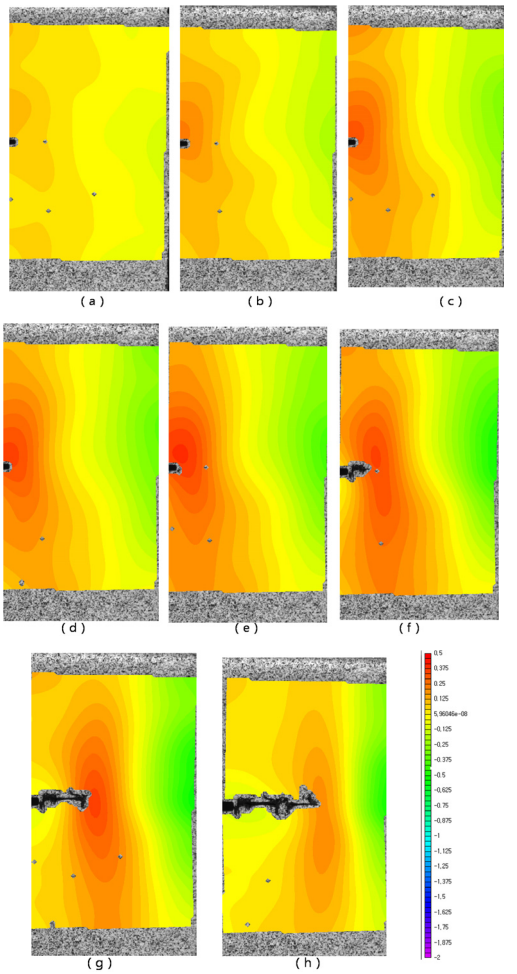

Figure 8: ϵ_{yy} strain contours obtained from the DIC analysis at the following load steps:(a)3th, (b)5th, (c)7th,(d)8th,(e)9th,(f)10th,(g)11th,(h)12th.

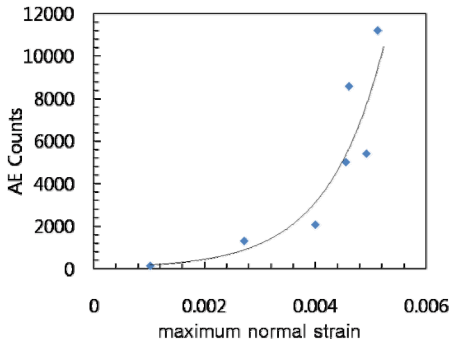

Figure 9: Relationship between the maximum normal strain and the AE count at each load step.

From the DIC analysis, we can find the normal strain ϵ_{yy} variation in the horizontal direction ahead of the notch tip. The strain at each load step is shown in Figure 10. The normal strains approached zero at a distance of 8mm from the crack tip. Also, the slope decreased more sharply in accordance with the loading.

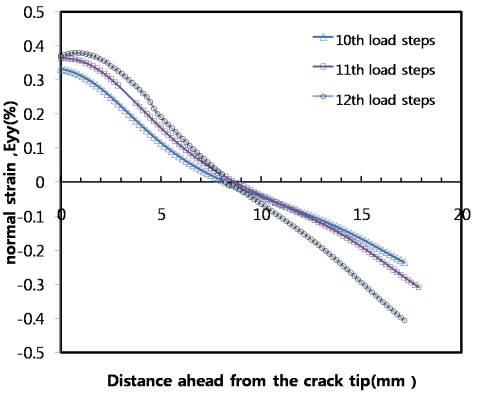

Figure 10: An example of ϵ_{yy} strain variation in x direction at a distance of 8mm from a crack tip.

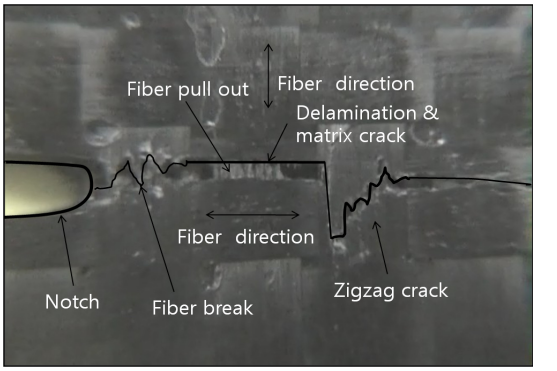

Figure 11: Damage and crack propagation path in a $\theta = 0^\circ$ type specimen.

The damage of a carbon fiber caused by cracking ahead of the notch tip is shown in Figure 11. The crack initiated from the notch tip and advanced in a zigzag fashion along the fiber direction because a

notch direction corresponded to the weft fiber direction. The accumulated AE count was relatively low until the 5th loading step.

In other words, damage to the fiber bundle and matrix accumulated from zero to the 5th or 6th loading step. After this step, the crack extended in a horizontal line. At the 9th step, the crack advanced in a zigzag fashion, following the broken fiber normal to the crack extension direction. The crack quickly added these zigzag advances to the long crack, and the AE count also increased, as shown in Figure 7. This extension aspect were repeated as the crack advanced.

4. Conclusions

The DIC method was proposed as a means of obtaining the displacement and strain of a CT specimen of a plain woven CFRP composite. The fracture AE count was also obtained, and was shown in relation to the strain obtained from DIC analysis, validating the present damage mechanism investigation. The results can be summarized as follows:

(1) The woven CFRP composite showed maximum tensile strength of the fiber because the fracture behavior was controlled by reinforcing fibers with high strength.

(2) The strain value obtained from the strain gauge measurement system and DIC were virtually identical.

(3) The relationship between AE counts and maximum normal strain ϵ_{yy} obtained from DIC analysis were determined, and represented the damage behavior effectively.

Acknowledgments

This work supported by Pukyong National University Research Abroad Fund in 2006(PS-2006-020), Korea.

References

[1] G. Lawcock and Y. Mai, "Progressive damage and residual strength of a carbon fiber enforced metal laminates", Journal of Composite Materials, vol. 31, no. 8, pp. 762-787, 1977.

[2] R. Harry and T. N. Massard, "An integrated micromechanics macro mechanics model for the prediction of the mechanical properties of woven materials", Proceedings of the International Conference on Composite Materials, pp. 267-270, 1991.

[3] F. Le'ne' and P. Paumelle, "Micro mechanism of damage in woven composite", Composite Material Technology ASME vol. 45, pp. 97-105, 1992.

[4] F. Gao, L. Boniface, S. L. Ogin, P. A. Smith and R. Greaves, "Damage accumulation in woven-fabric CFRP laminates under tensile loading", Composites Science and Technology, vol. 59, pp. 123-136, 1999.

[5] M. A. Sutton, W. J. Wolter, W. H. Peters, W. F. Ranson and S. R. McNeil, "Determination of displacement using an improved digital image correlation method", Image Vision Computer vol. 1, no. 3, pp. 133-139, 1983.

Author Profile

Oh-Heon Kwon

He received the B.E and M.E degree in Mechanical Engineering from Kyung-Pook National University in 1981 and 1983. He received Ph.D degree in Mechanical Engineering from the University of Tokyo (Japan) in 1991. He is currently a professor in Dept. of Safety Engineering at Pukyong National University in Busan. His research interests include damage evaluation for composite materials, acoustic emission and digital image correlation techniques.

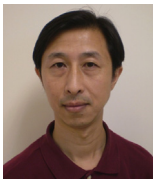

Shaowen Xu

He received the B.S and M.S degree in Engineering Mechanics from Huazhong University of Science and Technology (China) in 1985 and 1992. He received Ph.D degree in Mechanical Engineering from the University of South Carolina (USA) in 2003. He is currently a temporary Assistant Professor of METEET at the Georgia Southern University (USA). His research interests include multi-disciplinary and multi-scale modeling and simulations of engineering structures/systems and manufacturing processes.

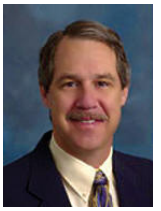

Michael Sutton

He received the B.S and M.S degree in Engineering Mechanics and Materials from Southern Illinois University in 1972 and 1974. He received Ph.D degree in Theoretical ANS Applied Mechanics from the University of Illinois (USA) in 1981. He is currently a Carolina Distinguished Professor of Dept. of Mechanical Engineering at the University of South Carolina(USA). His research interests include experimental mechanics, computer vision, digital image correlation and FEM of cracked bodies.